NUMERICAL INVESTIGATION OF SELF-WASTAGE PHENOMENA IN STEAM GENERATOR OF SODIUM-COOLED FAST REACTOR

Sunghyon Jang and Takashi Takata*
Division of Sustainable Energy and Environmental Engineering
Osaka University
2-1 Yamadaoka, Suita, Osaka, 565-0871 Japan
jang_s@qe.see.eng.osaka-u.ac.jp, takat_t@qe.see.eng.osaka-u.ac.jp

Akira Yamaguchi
The University of Tokyo
2-22 Shirakata, Tokai-mura, Ibaraki, Japan
yamaguchi@n.t.u-tokyo.ac.jp

Akihiro Uchibori, Akikazu Kurihara and Hiroyuki Ohshima
Japan Atomic Energy Agency
4002 Narita-cho, O-arai, Higashi-ibaraki, Ibaraki Japan, 311-1393
uchibori.akihiro@jaea.go.jp, kurihara.akikazu@jaea.go.jp, and ohshima.hiroyuki@jaea.go.jp

ABSTRACT

A small water leakage through a bleach at a heat transfer tube triggers Sodium-Water reaction (SWR) at the surface of the tube in a steam generator. If the SWR continues for some periods, the SWR will damage the surface of the defect so it will be enlarged. These phenomena are called Self-wastage. Numerical quantification of the self-wastage phenomena has been carried out using a computational code of multi-component multi-phase flow involving sodium-water chemical reaction: SERAPHIM. Numerical procedures are devised to evaluate the self-wastage phenomena. Thermophysical properties in a metastable condition are used to assess the wastage rate. Self-wastage evaluation was carried out by reconstructing the mesh grid which reflects the defect enlargement. As a benchmark analysis, 2-dimensional calculations are performed to evaluate the shaped and the width of the complete enlarged crack under the same condition of the SWAT experiment. Numerical results show good agreement with the experimental result in both the shape and the width of enlarged defect. The shape of enlarged defect has the funnel shape, and the enlarged width of the defect on sodium side was 4.72 mm which shows good agreement with the experimental data (4.96 mm).

KEYWORDS
Sodium-Water Reaction, Self-wastage phenomena, CFD, Sodium Faster Breeder Reactor

1. INTRODUCTION

Sodium-Water Reaction (SWR) description is an essential issue for safety design of steam generator in a Liquid Metal Fast Breeder Reactor (LMFBR). SWR takes place when water or vapor leak into sodium side through a crack in the heat transfer tube in a steam generator. If SWR continues around the initial crack, the deterioration of the tube wall is triggered by the corrosive reaction product such as sodium

* Footnote, if necessary, in Times New Roman font and font size 10

hydroxide (NaOH). Then a high-pressure water and vapor bring about the erosion of the weakened material. As a result, the crack can eventually enlarge to a size that allows a stable reacting jet [1]. This self-enlargement of the crack is called 'self-wastage phenomena.' It has the possibility that the increased resultant leak damage neighboring heat transfer tubes, it might lead to secondary failure. In 1987, 39 secondary tube leak occurred in a time of approximately 10 sec in the Prototype Fast Breeder Reactor Superheater 2 at Dounreay, UK [2]. These phenomena are made more important to model by the fact that small leaks (less than 0.005 g/sec) are not likely to be detected after steam generator fabrication neither they are likely to be detected during operation of an LMFR plant until the tube is significantly leaking (few g/sec). Since the most of initial crack starts from a micro-leak (less than 0.05 g/sec), evaluation of the leak evolution from micro-leak to leak is an imortant issue for detection capability and to improve safety of the SFR system.

Experimental studies on micro leak test have been studied to evaluate the self-wastage phenomena by several investigators. [3-7]. It was observed that the corrosion started from the sodium side and advanced to the steam side through the tube wall. Also, the leak rate stays almost unchanged until the thin edge of the tube wall is removed on the steam sides. Some empirical correlation between the self-wastage rate and experimental conditions such as sodium, steam temperature, initial and average leak rate were derived. However, the measuring technique, such as an each phase temperature and concentration of chemical species, is not enough mature to obtain data with high spatial resolution and accuracy. Also, many factors are related to the phenomena. Thus, an experimental approach is not sufficient to evaluate the self-wastage phenomena quantitatively. Accordingly, numerical quantification of thermal-hydraulic and chemical characteristics in the SWR is an alternative way for an approach to the SWR study.

In this study, we devised a numerical procedure to reproduce the self-wastage phenomena and evaluate the enlargement of the crack using a computational code of multi-component multi-phase flow involving sodium-water chemical reaction, SERAPHIM (Sodium watEr Reaction Analysis PHysics of Interdisciplinary Multi-phase flow) [8]. Multi-fluid and one-pressure models are applied for a multi-phase thermal-hydraulic analysis in SERAPHIM.

To validate the numerical evaluation of self-wastage phenomena, a benchmark analysis of SWAT-2 experiment was carried out in this study [9]. Two-dimensional numerical analysis was conducted under the same condition of SWAT-2 experiment to evaluate the shape and the width of an enlarged crack.

2. SELF-WASTAGE PHENOMENA ANALYSIS

2.1. Numerical Procedure

Sandusky explained the character of the failure of wall material in the process of the water-into-sodium leak self-development is schematically shown in Fig.1 [10]. Self-wastage starts from the sodium side and advances to the water side through tube wall. As a result of the failure zone propagation, even though the diameter of the leak channel increases, the amount of water leaking out is controlled by the diameter of the original defect which little changes on the water side. So the leak rate stays almost unchanged until the opening of the remaining strap diaphragm would start to increase as a result of a combined corrosion-erosion effect. Also, it takes a few hours even a few days until the failure zone propagation reaches the tube wall on sodium side. Thus, it requires heavy computational loads to carry out a transient calculation which cover the whole period of the phenomena. Since most of the time during the self-wastage propagation, leak rate does not change until the sudden enlargement of the leak caused by penetration of the tube wall. In other words, most of the time during the period of the self-wastage propagation, it can be assumed that the thermo-physical condition is in steady state. Thus, the local wastage rate can be evaluated using thermal properties that are obtained from the numerical calculation in steady state. The

self-enlargement of the crack is reproduced by replacing solid cells to fluid cells according to the wastage evaluation. Figure 2 shows a numerical procedure for the self-wastage phenomena.

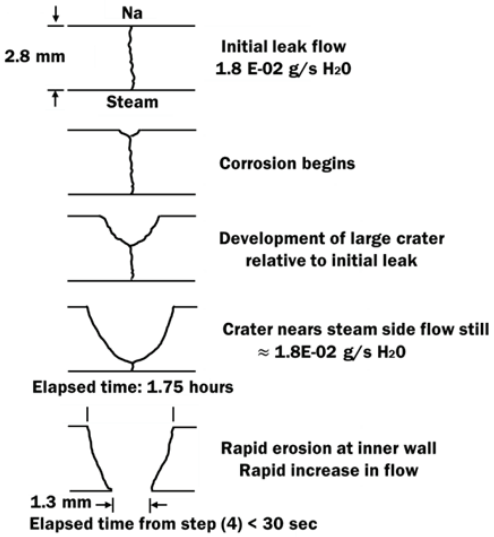

Figure 1. Process of enlargement by self-wastage

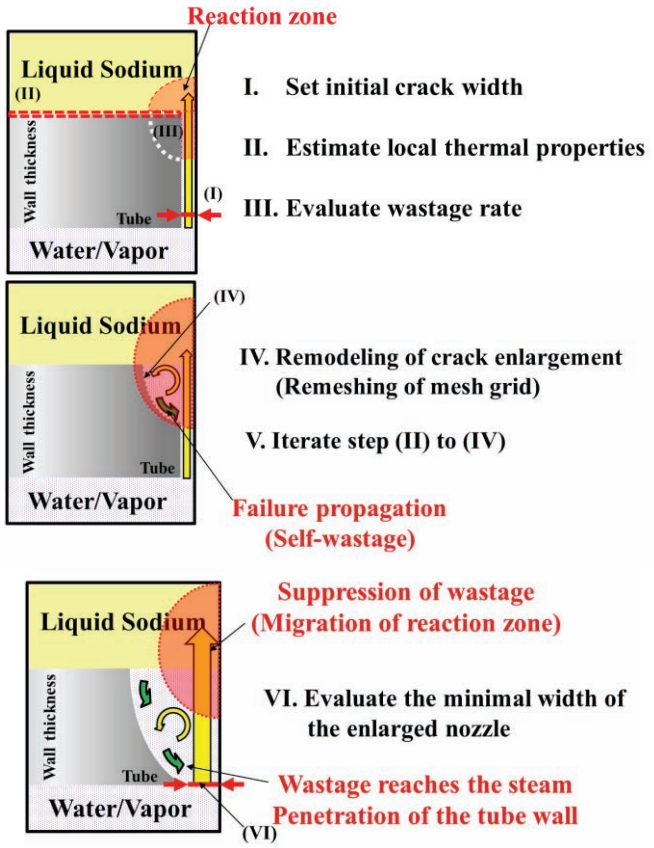

Figure 2. Numerical procedure for self-wastage analysis

(I) Set an initial crack width for the initial mesh grid
In the SWAT-2 experiment, a slit type crack was manufactured by pressing a square plate with drilled hole at the center of it. The crack was constant in the length of approximately 0.5 mm, and the width was in the range of 10 to 100 μm. For numerical calculation, initial crack is prepared to have a fixed width as a crack used in SWAT-2 experiment. Since the aspect ratio of the crack length and width is large, and the failure propagation is occurred along the crystal face of the material, it is assumed that the crack enlargement is expected to take place along the crack width and crack depth (tube wall thickness) direction. Thus, two-dimensional SWR is assumed as the analytical model.

(II) Investigation of local thermal properties
An unsteady numerical simulation is carried out for a particular period until it reaches metastable state. In order to estimate the wastage rate, we investigate temperature of the gas mixture and, sodium hydroxide concentration.

(III) Assessment of local wastage rate
The local wastage rate on the surface of the crack is evaluated according to the hypothetical Arrhenius model by using the mixture gas temperature and sodium hydroxide concentration

(IV) Reconstruction of the computational mesh that reflects crack enlargement
Reconstruction of the computational mesh grid is carried out by replacing the solid cells (tube wall) to fluid cells in the both crack width and depth direction on the surface of the tube wall. The amount of self-wastage is determined by the wastage rate which is calculated in step (III). More detailed about the local wastage evaluation and the reconstruction of the mesh grid are explained in the following sections. Then the step (II) to (IV) are repeated until the remaining thickness of the wall becomes 15% of the initial thickness. Since it was reported that when the remaining tube wall thickness become thinner than a specific level, the remained wall will be altered by the steam pressure and larger leak occurs. In this study, as a penetration condition 15% of the initial thickness is adopted from the viewpoint of Probabilistic Fracture Mechanics.

(V) Evaluate the minimal width of the enlarged crack
Since the crack width is enlarged, the leak rate will also increase, and it brings a migration of the reaction zone toward the sodium side. As a result, the corrosive reactant such as sodium hydroxide, seldom reaches the tube wall. Thus, the self-wastage phenomena will be mitigated. In this study, we will focus on the outside width of the enlarged leak from the viewpoint of conservative safety assessment.

2.2 Local Self-wastage Rate Estimation

Experimental approaches had been carried out to evaluate the self-wastage rate, and the following proportional equation was derived from related temperature with Equation (1).

$$WR \propto \exp\left(K_1 - \frac{K_2}{T} \right) \quad (1)$$

Where WR is wastage rate, K_1 and K_2 are constants and T is the absolute temperature of sodium and water/steam [11]. From the experimental result, it was demonstrated that the sodium hydroxide is the major product in the SWR from the viewpoint of thermo-chemical properties [12]. The influence of the sodium oxide is neglected since it would not frequently be generated because of its high-energy barrier. Therefore, physical amounts related to SWR and the wastage rate are gas temperature and sodium hydroxide concentration.

In this study, we adopted a hypothetical Arrhenius corrosive equation to describe the self-wastage rate.

$$WR = a\left[NaOH\right]^{b} exp\left(-\frac{c}{T}\right) \quad (2)$$

$$W = WR \cdot t = a\left[NaOH\right]^{b} exp\left(-\frac{c}{T}\right) \cdot t \quad (3)$$

Where *WR* is wastage rate [mm/sec], [NaOH] is sodium hydroxide concentration [kg/m^3], T is gas temperature and a, b and c are constants. Constant a is called the pre-exponential factor which is related to molecular collision. The units of the a are reciprocal seconds. The pre-exponential factor a is a constant that can be derived experimentally or numerically. However, it is hard to find a reliable experimental result regarding the pre-exponential factor, we decided to adopt the maximum amount of the wastage rate to ignore transient effect of the pre-exponential factor. The maximum wastage (WR) in each calculation is 20% of the tube thickness. Then constants a for the maximum local wastage is adopted to evaluate local wastage in other cells. For b and c, experimental results are adopted [13].

2.3 Reconstruction of a Computational Mesh Grid that Reflects Leak Enlargement

Reconstruction of a computational grid that reflects the leak enlargement is conducted by replacing solid cells to fluid cell according to the local wastage rate (amount).Example of wastage rate estimation and remodeling of computational mesh grid are depicted in Fig.3 [14]. It shows the estimated wastage line and initial crack surface. By replacing solids cells to fluid cells under the wastage line, new computational mesh grid which reflects the enlarged crack is obtained

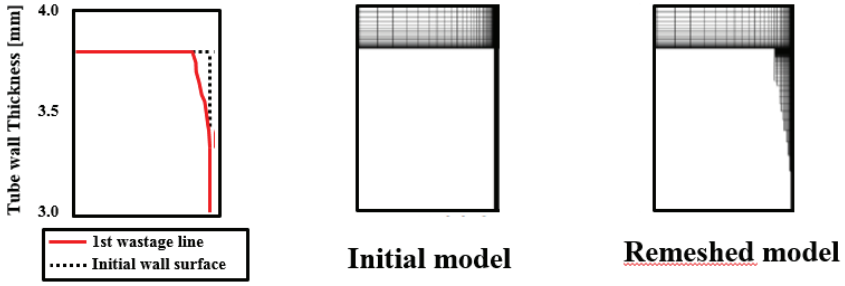

Figure 3. Reconstruction of computational mesh that reflect crack enlargement

3. NUMERICAL ANALYSIS AND RESULTS

3.1 Analytical Model and Conditions

Figure 4 and 5 show the analytical region and boundary conditions for the initial calculation. To reduce the calculation cost, asymmetric grid is adopted. The crack width, shape, and the tube thickness are decided to have same geometric shape with the SWAT-2 Experimental data [15]. The height of the computational grid was decided to have as three times as longer than the length of the injected reactant jet which is estimated by Dumm's equation. [16]

Table 1 shows the experimental conditions of the SWAT-2 that was also used as boundary conditions for the numerical calculation [17]. The crack width in the mesh grid (7.5μm) was decided to be divided equally into four cells after considering the effect of the mesh resolution. The minimum height of the mesh grid was 10μm, and the whole mesh grid was divided into 49 (I) ×107 (J). For the inlet boundary

condition, constant volume rate (2.5×10^{-5} g/s: average leak rate in the experiment) was adopted. Time step was 1.0×10^{-9} sec.

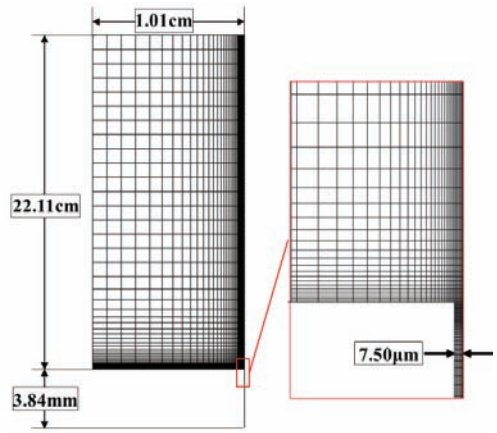

Figure 4. Analytical region for initial calculation

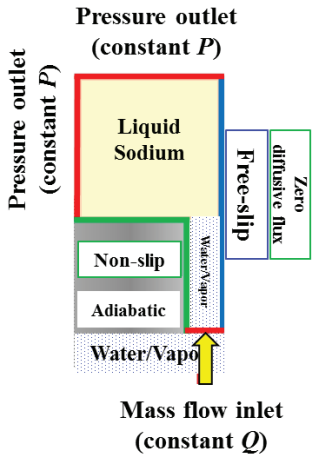

Figure 5. Boundary conditions for numerical calculation

Table 1. SWAT-2 Experimental conditions

Experimental Conditions	
Experiment Number	: 2020
·Tube Material	: 2.25 Cr-1Mo
·Tube Thickness	: 3.84 mm
·Sodium Temperature	: 470 °C
·Sodium Pressure	: 1.47×10^{-1} MPa
·Steam Temperature	: 470 °C
·Steam Pressure	: 12.8 MPa
·Initial crack width	: 15 μm
·Initial leak rate	: 3.4×10^{-4} g/s
·Average leak rate	: 2.5×10^{-5} g/s

3.2 Initial Calculation

Figure 6 shows the gas volume fraction and vector distributions around the outside of the crack until 2.0×10^{-1} sec. At 1.0×10^{-3} sec, swirl is developed around the exit. The diameter of the first swirl is about 1.0 mm, this swirl expanded toward downstream until 1.0×10^{-2} sec, the size of the swirl became bigger until it reaches the size of 2.0 mm (width) ×4.0 mm (height). As the initial swirl flow to downstream, new swirl is created around the crack exit and the size became 1.0 mm of width. This new swirl moved also to downstream, and another swirl is generated again on the outside of the crack. The swirl velocity is 5 m/s.

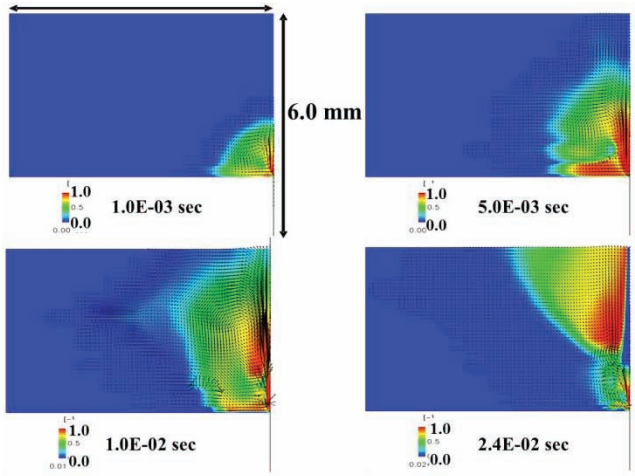

Figure 6. Gas volume fraction

Figure 7 shows the gas temperature, NaOH concentration around the crack exit and these distributions at the surface of the tube at 3.0×10^{-2} sec. Very high temperature (above 1200 °C) appears downstream of the crack along the injected flow, and relatively high temperature is observed at the surface of the tube around the crack exit. At the same place, relatively high NaOH concentration appears. The distribution of the gas temperature and NaOH concentration shows that these properties are changing with time elapsed.

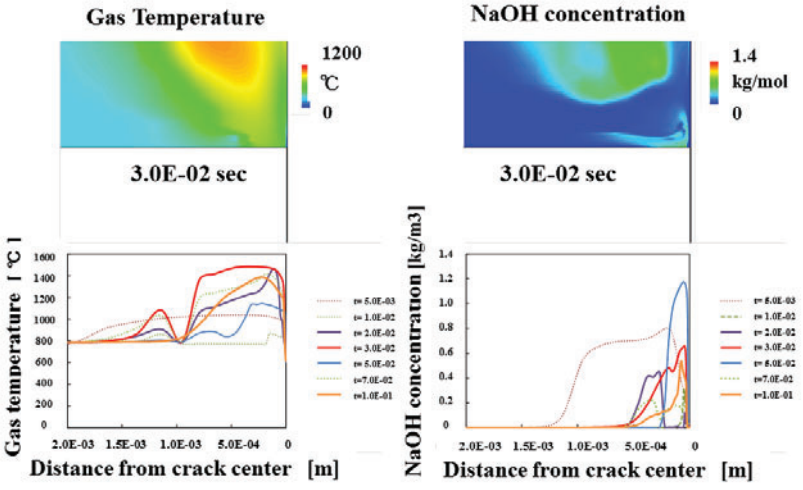

Figure 7. Gas temperature and NaOH concentration at crack exit

To investigate transient aspect of the gas temperature and NaOH concentration at the surface of the tube, these properties on a specific mesh are obtained as shown Fig. 8. It shows that these two properties are fluctuating within a certain range from 0.1 sec with time advance. Since leak rate stays almost unchanged in the most of the time during the self-wastage propagation, thus it is assumed that these thermo-physical properties also have a uniform (or steady) pattern. As a result, it can be expected that the self-wastage advance through the wall with a constant rate. Thus, it can be assumed that the pattern, which the properties has in fig. 8, lasts with time advance. Therefore, in order to dismiss the transient change of thermal properties, the mathematically averaged properties (until 1.2 sec) of gas temperature and NaOH concentration are used to estimate the self-wastage rate.

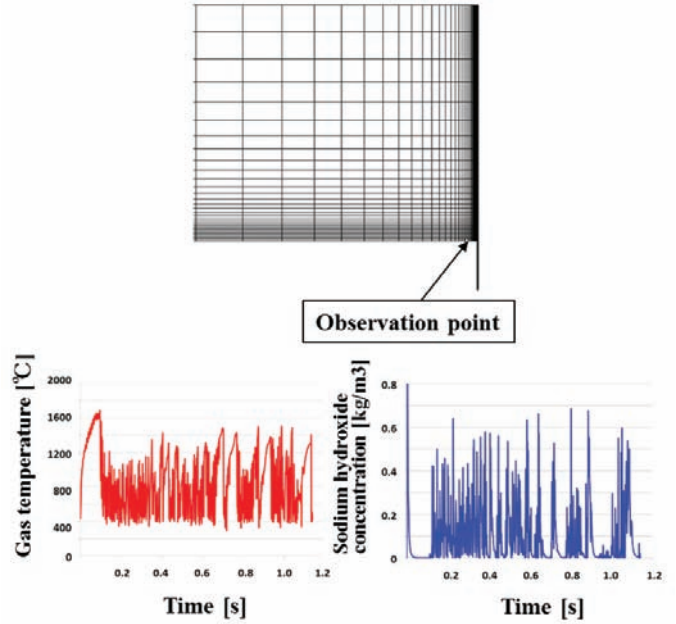

Figure. 8 Gas temperature and NaOH concentration on a single mesh

3.3 Secondary Calculation with the Computational Mesh Reflecting Leak Enlargement

The amount of enlarged depth and width of the tube is evaluated based on Self-wastage rate equation 2 using the averaged properties obtained in the previous chapter. B and C constants are referred the NaFeO wastage experiment which was carried out by JAEA. The maximum amount of the enlarged depth and width at each calculation are arbitrarily limited to 20% of the initial tube thickness.

A new analytical mesh grid is constructed by replacing solid cells to fluid cells on the surface according to the wastage rate as shown in Fig. 9. Further numerical calculation is carried out using this new mesh grid under the same condition as the former calculation. The inside of the crack is regarded as being filled with the steam.

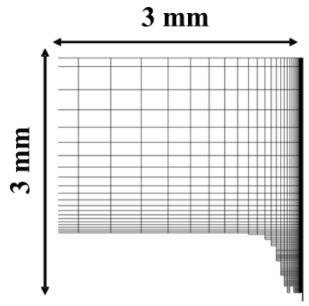

Figure. 9 Reconstruct mesh that reflects crack enlargement

Figure 10 shows the gas fraction, gas temperature and NaOH concentration around the crack exit at 3.0×10^{-2} sec. As shown in Fig.9, injected steam is expanded toward the downstream. In the enlarged crack area, gas phase is filled. The swirl is generated between the enlarged crack wall and the mainstream of the injected crack. It brings reaction product to the wall. Thus, relatively high temperature also appears near the enlarged crack surface. Regarding NaOH concentration, it is also showed that NaOH is created and stored in the area. Therefore, it is also expected that the failure propagation would proceeds in the both direction.

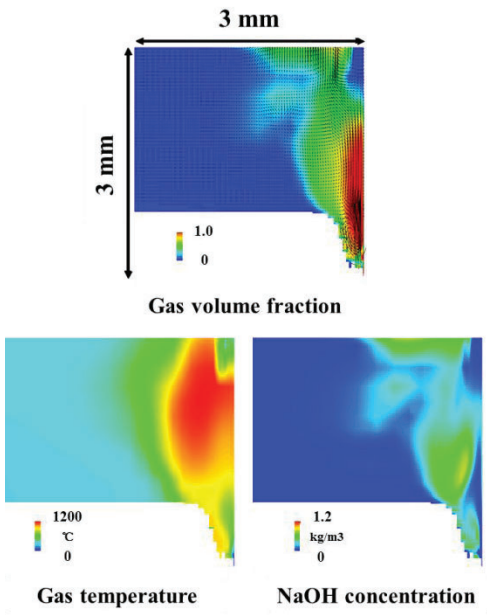

Figure. 10 Physical properties around the enlarged crack (t = 2.0×10^{-2}sec)

For further evaluation, physical properties are obtained on the surface of the enlarged crack. Figure 11 shows transient properties of the gas temperature and NaOH concentration at arbitrary four points among the mesh points on the surface of the crack. Gas temperature at the four points decrease until 1.5×10^{-2} sec and increase about 1200 $^{\circ}$C then are kept at above 1000°C with some changes. NaOH concentration shows different tendency that the concentration increases until 1.5×10^{-2} sec then rapidly decreases and are kept below 0.8 with some fluctuations. These properties fluctuations are brought by the swirl that is generated by the injected jet. For further evaluation, a new computational mesh grid which reflects further crack enlargement are reconstructed based on the local self-wastage rate which is obtained by the local thermal properties.

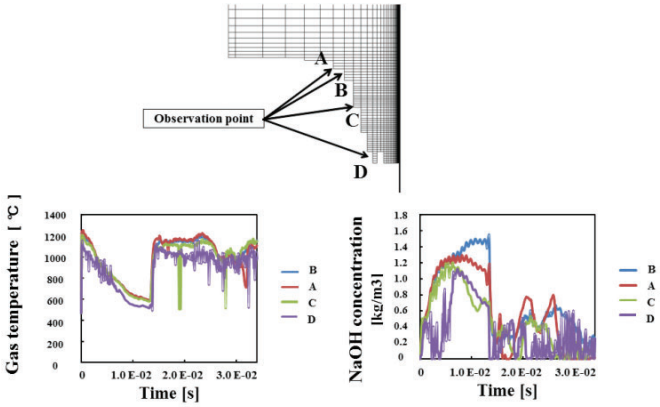

Figure. 11 Physical properties obtained at 4 different meshes

3.4 Failure Propagation

Further numerical calculation is carried out using the analytical grid in Fig. 12. Figure 12 shows the high temperature and highly condensed NaOH exist on the wall in the steam side. By taking the average gas temperature and NaOH concentration at the surface of crack, local wastage rate is estimated. Based on these local wastage rates, again the 3rd analytical grid is created. Like the same manner, the 4th and 5th analytical mesh grid are generated and shown in Fig. 13. It shows that the failure propagation proceeds to the water side through crack center.

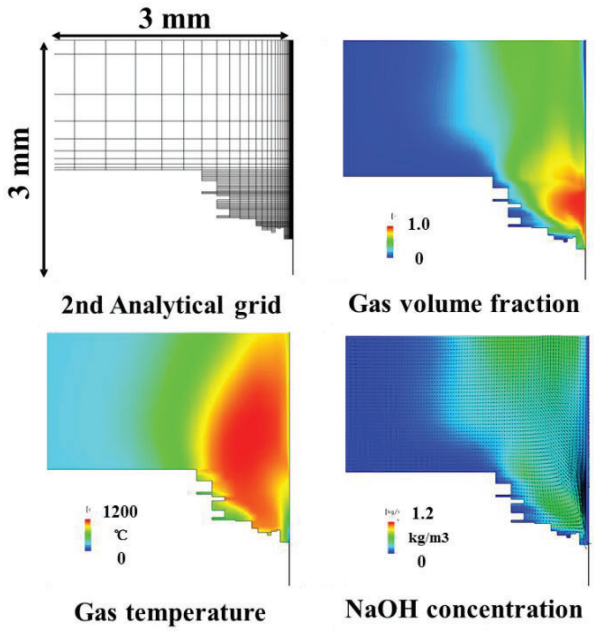

Figure. 12 2nd analytical grid and physical properties around crack exit (t = 2.0×10^{-2}sec)

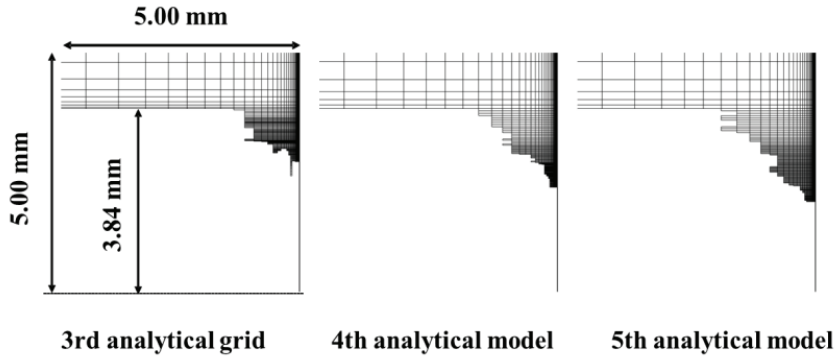

Figure. 13 3rd, 4th and 5th analytical grid and failure propagation

Figure 14 – (a) shows the 6th analytical grid and the physical properties around the enlarged crack. As shown in the figure, the high temperature and NaOH concentration do not reach the deeper wall on the crack surface in the width direction. Therefore, the surface of the wall would become a smooth surface, and it is expected that the failure propagation would advance dominantly in the crack depth direction. The 9th analytical region and the physical properties around the crack are shown in Fig.14-(b). Figure 14-(b) shows the 9th analytical grid and the physical properties around the enlarged crack. As shown in the figure, the crack enlargement takes place dominantly in crack depth direction. Since the crack enlarged in the width direction, the injected jet and its reaction product are transported along the downstream and do not reach the crack wall in the upper region. Therefore, the self-wastage phenomena do not affect on the wall in this region. The leak enlargement would proceed to the steam side through the crack wall. As mentioned earlier in the section.2.1, after estimating the wastage rate and reproducing the analytical grid are performed until the thickness of the remaining tube wall become 15% of the initial thickness. On the other words, when the failure propagation advances 85% of the initial tube wall thickness, it is assumed that the remaining diaphragm would be removed by the jet pressure thus the tube is penetrated. The penetrated mesh grid was shown in Fig.15. The cross section of the enlarged crack is a funnel shape that has larger opening on the sodium side. Estimated outer with of the crack is 2.36 mm, and the inner one was 0.09mm.

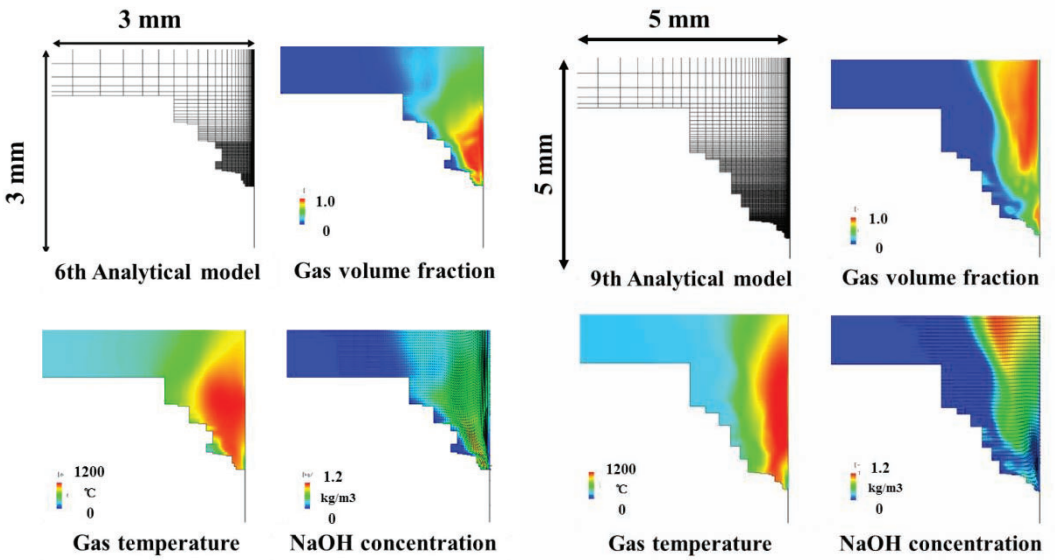

(a) 6th Mesh gird (b) 9th mesh grid

Figure. 14 Analytical grid and physical properties around crack (t = 2.0×10^{-2}sec)

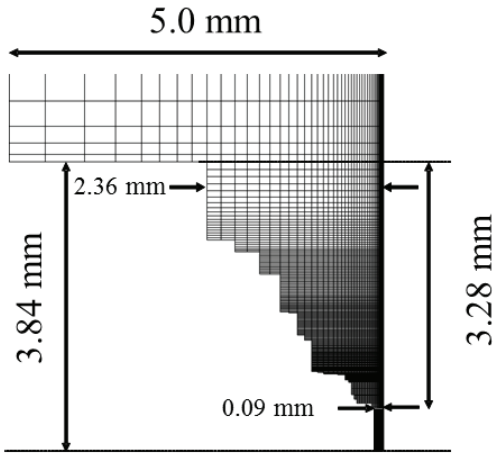

Figure. 15 Mesh grid of penetrated crack

The comparison of the shape of the enlarged crack between the numerical result and the SWAT-2 experiment result is shown in Fig. 16. Both of the results of the enlarged crack have funnel-shaped cross section. The outer and inner diameter (width) of the penetrated crack of SWAT-2 experiment was 4.96 mm and 0.54 mm, respectively. The crack shape on the outside shows agreement between the present result and the experimental result. However, as regard the crack width on steam side have difference between the two results. To increase accuracy regarding the failure propagation in the crack depth direction, refinements about the remeshing process are necessary.

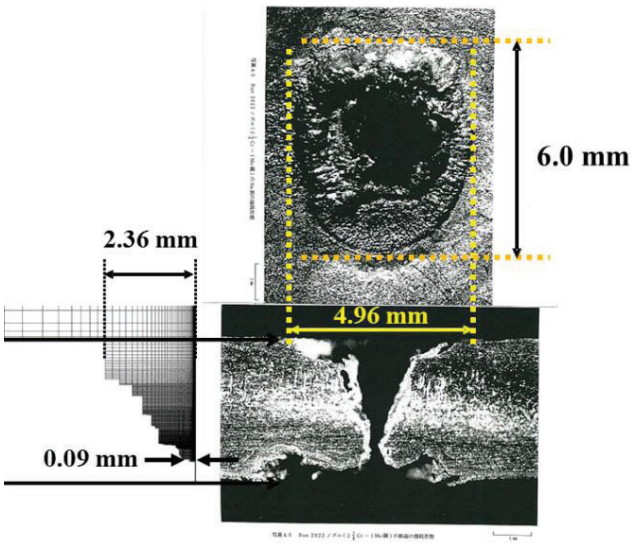

Figure. 16 Comparison of the enlarged crack by numerical simulation and experiment

In Figure 17, local wastage rates toward the crack thickness and width direction are compared. Accumulated wastage rate toward the both directions are marked according to non-dimensional time which indicates the number of the repetition of the calculations. The non-dimensional number is

represented by dividing repeated number of calculation by the total number of calculation which is 10 in the present study. Figure 17 indicates that the wastage rate increasing speed toward the nozzle thickness direction is higher than that of the nozzle width direction. It suggests that the width of enlarged nozzle is determined according to the thickness of the nozzle and the self-wastage rate toward the thickness direction. Also the upper limit of the width of the enlarged nozzle would be evaluated when the wastage rate is known.

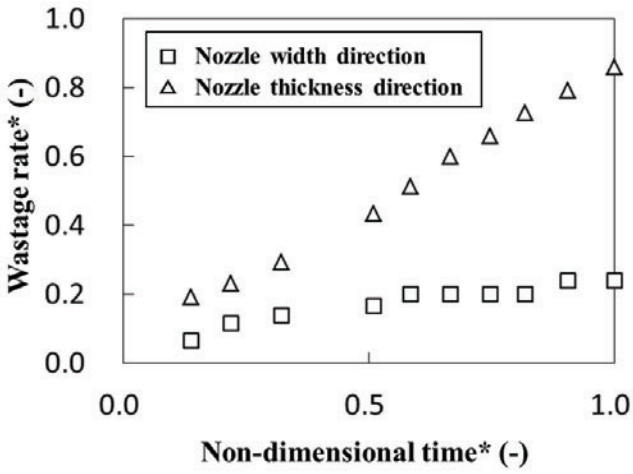

Figure. 17 Wastage rate in nozzle width direction and thickness direction

4. CONCLUSIONS

Numerical evaluation model of the self-wastage phenomena and failure propagation have been devised, a benchmark numerical calculation has been carried out to validate the numerical model. In the study, the shape of the enlarged crack is evaluated.

Five-step procedure are devised and carried out to reproduce the transient phenomena of self-wastage and the failure propagation. At first a numerical calculation is carried out with analytical mesh grid which has a single-width crack. As a result of the calculations, it is demonstrated that the injected steam reacted with liquid sodium and brings sodium water reaction around outside of the crack. High temperature and highly NaOH-condensed exist on the surface of the wall. Averaged gas temperature and NaOH concentration on the surface of the crack are obtained. Wastage rate is estimated based on Arrhenius hypothetical model by using the gas temperature and the NaOH concentration. Then replacing the solid cells to fluid cells are conducted on the surface of the crack according to the wastage rate estimation. As a result, new-analytical mesh grid is generated to have the enlarged crack. Using this new mesh grid, the above same procedures are carried out as the failure propagation proceeds to 85% of the initial tube thickness. When the remained thickness of the tube becomes 15% of the initial thickness, it is regarded that the tube is penetrated, and the outer and inner width of the crack are estimated.

It is demonstrated that the self-wastage phenomena starts from the sodium side and advance through the tube wall. The present results show the enlarged crack width on the sodium side is 4.72 mm and the cross section shape of the enlarged crack is funnel-shaped. These results show good agreement with SWAT-2 results regarding the enlarged crack width (4.96 mm) on the sodium side and the shape. The numerical benchmark analysis demonstrates the applicability of the self-wastage evaluation model to evaluate the self-wastage phenomena.

It is also found that the self-wastage rate differs according to the direction. Self-wastage rate in the crack depth direction is higher than that in the crack width direction. Therefore, there will be a limitation regarding the maximum width of the enlarged crack.
This study demonstrates the feasibility of evaluation of the failure propagation by the self-wastage phenomena through numerical procedure.

REFERENCES

1. H. H. Neely and C.E. Boardman, "Status of U.S. studies of failures and failure propagation in steam generator", *Proc.IAEA/IWGFR specialists' Meeting on Steam Generator Failure and Failure Propagation Experience,* Aix-en-Provence, France , September 26-28, 1990.
2. R. Currie, G.A.B Linekar and D.M. Edge, "The Under Sodium Leak in the PFR Superheater 2 in February 1987 ", *Proc. IAEA/IWGFR specialists' Meeting on Steam Generator Failure and Failure Propagation Experience,* Aix-en-Provence, France, September 26-28, 1990.
3. D.A. Green, "Small Leak and Protection Systems in Steam Generators", *Int. Conf. on Liquid Metal Technology i n Energy Production,* Seven Springs, PA, USA, May, 1976.
4. D. W. Sandusky, "Small Leak Shutdown, Location and Behavior in LMFBR Steam Generators", *Int. Conf. on Li quid Metal Technology in Energy Production*, Seven Springs, PA, USA, May 1976.
5. F.A. Kozlov, "Studies on Some Problems of Leaks in Sodium-Water Steam Generator", *Int. Conf. on Liquid Met al Technology in Energy Production,* Seven Springs, PA, USA, May, 1976.
6. J.Y. Jeong, T.Kim, J.Kim, B,Kim and N.Park, "Analysis of Micro-Leak Sodium-Water reaction phenomena in a Sodium-Cooled Fast Reactor Steam Generator." *Korean J. Chem. Eng.,***vol. 26**, pp. 1004-1008, (2009).
7. M. Kuroha, K. Sasaki, H. Kawabe, T. Yamada and M. Sato, "Study of Micro-Defect Self-Wastage Phenomena o n LMBR Prototype Steam Generator's Tube." PNC TN941 82-101, Power Reactor and Nuclear Fuel Developm ent Corporation (1982).
8. T. Takata and A. Yamaguchi, "Numerical Approach to the Safety Evaluation of Sodium-Water Reaction," *J. Nuc l. Sci. Technol*., **vol. 40**, pp. 708-718, (2003)
9. M. Kuroha, K. Sasaki, H. Kawabe, T. Yamada and M. Sato, op. cit.
10. D. W. Sandusky, op. cit.
11. M. Hori, "Sodium/Water Reactions in Liquid Metal Fast Breeder Reactions," *Atomic Energy Review*, **vol.** 183, p p.707-778, (1980).
12. Y. Okano, "Numerical simulations study on sodium-water reaction (4): Theoretical adiabatic temperature of sodi um-water reaction zone, " *Preprints 2001 Ann. Meet. of Atomic Energy Society of Japan*, I4, 2001.
13. A. Kurihara, R. Umeda, S. Kikuchi and H. Ohsima, "Study on Sodium-water Reaction Phenomena in Steam Ge nerator of Sodium-cooled Fast Reactor (6) Thinning Evaluation due to High-temperature Sodium-hydroxide Im pinging Experiment. ", *Atomic Energy Society of Japan 2011 Autumn meeting*, P-09, Kitakyusyu, Japan, Sep. 1 9-22, 2011.
14. Y. Onish, T. Takata, A. Yamaguch, A. Uchibori, S. Kikuchi, A. Kurihara and H. Ohshima, "Numerical Approach of Self-Westage Phenomenon in Steam Generator of Sodium-Cooled Fast Reactor", *8th Japan-Korea Symposiu m on Nuclear Thermal Hydraulics and Safety*, N8P1070, Beppu, Japan, December 9-12, 2012.
15. M. Kuroha and K. Shimoyama, "Micro-Leak Behavior on LMFBR Monju Steam Generator Tube Materials – St udies of Micro-leak Sodium-Water Reaction, PNC ZN9410 86-027, Power Reactor and Nuclear Fuel Developm ent Corporation (1982).
16. K. Dumm, "Small Water/Steam Leaks in Sodium-Heated Steam Generators," *IAEA Study Group Meeting on Ste am Generators for LMFBRs*, Summary Report IAEA IWG FR/1 Bensberg, (1974).
17. M. Kuroha, K. Sasaki, H. Kawabe, T. Yamada and M. Sato, op. cit.